

A Ruthenium–Rhodamine Complex as an Activatable Fluorescent Probe

Josefina del Mármol, Oscar Filevich, and Roberto Etchenique*

Departamento de Química Inorgánica, Analítica y Química Física, INQUIMAE, Facultad de Ciencias Exactas y Naturales, Universidad de Buenos Aires, Ciudad Universitaria Pabellón 2 AR1428EHA Buenos Aires, Argentina

We describe the synthesis and characterization of a ruthenium–bipyridyl complex bearing a rhodamine-based fluorescent ligand. The complex is weakly fluorescent due to the quenching of rhodamine. Upon irradiation of the MLCT band it releases rhodamine in a fast and clean heterolytic reaction, increasing its fluorescence nearly 6-fold and making it the first visible-light activatable fluorophore based in transition metal chemistry. These properties and its lack of toxicity make it a good candidate for its use as a biologically friendly caged fluorescent probe. The use of this probe as a neuronal marker, and as a flow profiler in a thin, planar cavity and in a model flow injection analysis (FIA) is demonstrated.

Fluorescent probes are among the most important chemical tools in use in analytical chemistry. Their applications range from the typical cuvette fluorimetric analysis to advanced methods such as ultrafast DNA sequencing,¹ microfluidic-based high throughput cell sorting,² 2D/3D measurement of physicochemical properties such as pH³ and temperature,^{4,5} detection and quantification of chemical species,⁶ etc.

Fluorescent probes are usually active in its native molecular form but sometimes, a probe will change its emission properties after it has been chemically modified by the system under study. An example of this strategy is the use of esterified, fluorescent, Ca²⁺ cytosolic indicators, which can pass through the membrane due to its lipophilicity, being cleaved to their carboxylic acid form by means of cellular esterases, and become active Ca²⁺ indicators, useful to detect changes in neurons and other excitable cells.⁷

Caged compounds, also named phototriggers, are widely used in chemical and biological research.⁸ In the latest years a number of photolabile protecting groups have been developed for the

caging of a variety of biomolecules including neurotransmitters,⁹ second messengers,¹⁰ gene inducers,¹¹ small peptides,¹² etc.

A caged fluorescent probe is a molecule which is weakly fluorescent or not fluorescent at all in its native form, but becomes fluorescent upon irradiation with light of the proper wavelength. This behavior makes it possible to activate the probe in very specific parts of the system under study, while leaving the remaining probe molecules in their inactive, nonfluorescent form. Uncaging of the caged probe can be done in very small parts of a tissue, in a single cell, or in a specific subcellular compartment, while direct injection of the probe in such a small volume would be impossible. A caged fluorescent probe would turn up useful for example, in cell-lineage tracing and fate mapping in developmental biology studies, in the microfluidics research of analytical systems,¹³ etc.

If the irradiation wavelength needed for uncaging of the caged, quenched probe is different from the irradiation wavelength leading to fluorescence of the free, active probe, then the uncaging process is said to be *orthogonal* to the fluorescence process, and fluorescence can be activated and detected without interference. On the other hand, if both wavelength ranges overlap, some activation can occur during the monitoring process. A quasi-orthogonal probe can be obtained if the amount of light needed for activation is much higher than that needed for a proper emission, that is: $\epsilon_{\text{PU}}\phi_{\text{PU}} \ll \epsilon_{\text{EM}}\phi_{\text{EM}}$, where ϵ_{PU} is the molar extinction of the band leading to photouncaging, ϕ_{PU} is the quantum yield of photouncaging, ϵ_{EM} is the molar extinction for the probe excitation and ϕ_{EM} the emission quantum yield of the free probe.

In recent work we have presented the use of metal complexes as photolabile protecting groups for biomolecules, unveiling an entire new family of caged compounds based in coordination chemistry. Since the first member of this family was presented¹⁴ we have demonstrated the usefulness of this strategy devising caged amines, including the neurotransmitters serotonin¹⁵ and

* To whom correspondence should be addressed. E-mail: rober@qi.fcen.uba.ar.

- (1) Scherer, J. R.; Kheterpal, I.; Radhakrishnan, A.; Ja, W. W.; Mathies, R. A. *Electrophoresis* **1999**, *20*, 1508–1517.
- (2) Wolff, A.; Perch-Nielsen, I. R.; Larsen, U. D.; Friis, P.; Goranovic, G.; Poulsen, C. R.; Kuttera, J. P.; Tellemann, P. *Lab Chip* **2003**, *3*, 22–27.
- (3) Tang, B.; Yu, F.; Li, P.; Tong, L.; Duan, X.; Xie, T.; Wang, X. *J. Am. Chem. Soc.* **2009**, *131*, 3016–3023.
- (4) Lou, J.; Hatton, T. A.; Laibinis, P. E. *Anal. Chem.* **1997**, *69*, 1262–1264.
- (5) Filevich, O.; Etchenique, R. *Anal. Chem.* **2006**, *78*, 7499–7503.
- (6) Mao, J.; Heb, Q.; Liu, W. *Talanta* **2010**, *80*, 2093–2098.
- (7) Alonso, M. T.; Barrero, M. J.; Michelena, P.; Carnicero, E.; Cuchillo, I.; García, A. G.; García-Sancho, J.; Montero, M.; Alvarez, J. *J. Cell. Biol.* **1999**, *144*, 241–254.
- (8) Deiters, A. *ChemBioChem* **2010**, *11*, 47–53.

- (9) Gug, S.; Charon, S.; Specht, A.; Alarcon, K.; Ogden, D.; Zietz, B.; Léonard, J.; Haacke, S.; Bolze, F.; Nicoud, J. F.; Goeldner, M. *ChemBioChem* **2008**, *9*, 1303–1307.
- (10) Kantevari, S.; Hoang, C. J.; Ogrodnik, J.; Egger, M.; Niggli, E.; Ellis-Davies, G. C. R. *ChemBioChem* **2006**, *7*, 174–180.
- (11) Young, D. D.; Deiters, A. *Angew. Chem.* **2007**, *119*, 4368–4370.
- (12) Petersen, S.; Alonso, J. M.; Specht, A.; Duodu, P.; Goeldner, M.; del Campo, A. *Angew. Chem.* **2008**, *47*, 3192–3195.
- (13) Ross, D.; Johnson, T. J.; Locascio, L. E. *Anal. Chem.* **2001**, *73*, 2509–2515.
- (14) Zayat, L.; Calero, C.; Alborés, P.; Baraldo, L.; Etchenique, R. *J. Am. Chem. Soc.* **2003**, *125*, 882–883.
- (15) Zayat, L.; Saliermo, M.; Etchenique, R. *Inorg. Chem.* **2006**, *45*, 1728–1731.

GABA,¹⁶ and also the major excitatory neurotransmitter glutamate.¹⁷ Caged compounds based in ruthenium–bipyridyl chemistry show many advantages over traditional phototriggers, being activatable with low energy visible photons (down to 532 nm) and undergoing very fast kinetics, with reaction time constants in the order of tens of nanoseconds.¹⁸

In this work we present a caged fluorescent probe based on a ruthenium–bipyridine core, bearing a modified rhodamine as ligand. This complex behaves as a caged fluorescent probe, increasing its fluorescence around 6 fold upon visible light excitation, and providing a starting platform from which similar photoactivatable fluorescent probes can be engineered. We used the probe to visualize flow in capillary flow injection analysis (FIA) tubes and in 2D thin, planar cavities under repetitive stimulation using a laser diode and continuous high frequency video microscopy recording.

EXPERIMENTAL SECTION

All reagents were purchased from Sigma-Aldrich and used as received. Ru(bpy)₂Cl₂ was synthesized according to the literature using water as solvent.¹⁹ UV–Vis spectra were taken with a HP8453 diode-array spectrometer. NMR spectra were obtained using a 500 MHz Bruker AM-500. Fluorescence emission measurements were made with a PTI Quantamaster spectrofluorometer, corrected for the instruments response function. Rhodamine B was used as fluorescence standard of emission quantum yield ($\phi = 0.31$ in aqueous solutions). Quantum yield of the complex was obtained directly from the ratio of the spectral areas, which present the same shape.

The photouncaging quantum yield measurements were performed with a Nd:YAG diode pumped solid state laser doubled to 473 nm with a constant power of 6.3 mW. The light was collimated and sent through an optical path of 1 cm into a fluorescence glass cuvette, with stirring. Total irradiation energy was measured using a Coherent Fieldmaster FM light meter with a visible light photodiode model SR45.

Microscopy of leech (*Hirudo medicinalis*) ganglia was performed in a custom-made setup for photoelectrophysiology equipped with a micromanipulator used to impale the neuron body with the $\sim 1 \mu\text{m}$ tip diameter capillaries, and a CCD webcam as a registering device. An isolated leech ganglion from a segment between 7 and 14 was pinned down in a sylgard-coated, 35 mm Petri dish. Retzius cells were identified by their position, size, and firing behavior. Intracellular recordings were obtained with $\sim 20 \text{ M}\Omega$ sharp capillary microelectrodes, a Neuroprobe 1600 (A-M Systems) amplifier and a A/D signal acquisition board at 1 kHz sampling rate and custom-made software. For iontophoretic injection of the dye the microelectrode was filled with recording solution to which 1 mM caged fluorescent dye (chloride form) was added. Square, biphasic pulses of 1 nA, 2 Hz were applied for less than 5 min.

Images of thin spectrophotometric flow cells and FIA capillaries were performed using a Nikon TS-100 with a fluorescence adapter.

A consumer-electronics type compact digital camera (Casio Exilim EX-FC100) focusing through a normal eyepiece through a custom adapter was used to register the videos at ISO 800 sensitivity. Videos and image analysis were done using public access ImageJ software. Activation of fluorescence was performed with a 405 nm 6 mW laser diode was controlled with a pulse generator using a fast Reed relay to provide 20 ms light pulses. The laser beam was focused at the cell plane and monitored with an inverted microscope (Nikon TS-100 w/fluorescence adapter).

Syntheses. *Rhodamine B–Methylaminopropionitrileamide (RhodB–MAPN)*. 550 mg of rhodamine B.HCl were dissolved into 10 mL of dry 1,2 dichloroethane. The system was purged with N₂ and 300 μL of phosphorus oxychloride were added. The mixture was refluxed during 5 h. The solvents were distilled under a vacuum and the solid was immediately dissolved in dry acetonitrile. 500 μL of triethylamine and 108 μL of *N*-methylaminopropionitrile were added, and the mixture was refluxed during 12 h. The solvent was removed under a vacuum, redissolved in water, filtered to eliminate any solids and precipitated by addition of excess KPF₆. The dark red solid was washed several times with distilled water and dried over silica gel. Exchange of Cl for PF₆ in order to have a water-soluble ligand was performed by stirring overnight a 1:1 acetone–water solution of RhodB–MAPN.PF₆ with Dowex 22 anionic resin and lyophilizing the obtained solution. RhodB–MAPN chloride salt is somewhat hygroscopic and must be stored in a moisture free environment.

Overall yield: 55%. ¹H NMR (Acetone-d₆): ¹H δ 1.37 (t, 12H), 2.37 (t, 2H), 3.16 (s, 3H), 3.53 (t, 2H), 3.80 (m, 8H), 6.98 (d, 2H), 7.20 (dd, 2H), 7.37 (dd, 2H), 7.62 (m, 1H), 7.77 (m, 1H), 7.82 (t, 2H).

[Ru(bpy)₂(L)Cl]PF₆. For L = *Rhodamine B–Methylaminopropionitrileamide*. Twenty mg of Ru(bpy)₂Cl₂ were suspended in 2 mL of a 2:1 EtOH/water mixture and the suspension was heated to 80 °C until total dissolution. The formation of the [Ru(bpy)₂(H₂O)Cl]⁺ complex was determined by its absorption band at 490 nm (in water). After formation of the chloro–aquo complex, two equivalents of the RhodB–MAPN chloride salt were added, and the reaction was followed by TLC using silica plates and a mixture of 1:1:1 water/EtOH/nBuOH as eluent. The solution was heated at 80 °C during about 2 h, until no further TLC changes were observed. All the following procedures were done in darkness. The solution was filtered to remove any insoluble particles and the solvent was removed under a vacuum. The obtained oil was redissolved in 4 mL of a 3:1 acetone:methanol mixture and was precipitated by addition of excess THF.

The THF fraction containing unreacted ligand was discarded, and the precipitate was washed several times with THF, redissolved in water and precipitated with saturated KPF₆. Yield: 26%. NMR (Acetone-D₆): ¹H δ 1.35 (m, 12H), 2.98 (t, 2H), 3.10 (s, 3H), 3.40–3.55 (dm, 2H), 3.80 (m, 8H), 6.97 (d, 2H), 7.20–7.40 (m, 6H), 7.60 (d, 1H), 7.67 (t, 1H), 7.70–7.85 (m, 4H), 7.88–7.98 (m, 4H), 8.17 (t, 1H), 8.30 (t, 1H), 8.56 (dd, 2H), 8.69 (d, 1H), 8.72 (d, 1H), 9.55 (d, 1H), 10.08 (d, 1H).

For L = *Vinylacetoneitrile (VACN)*. Twenty mg of Ru(bpy)₂Cl₂ were suspended in 2 mL of 96% EtOH, and the suspension was heated at 80 °C until total dissolution. The formation of the

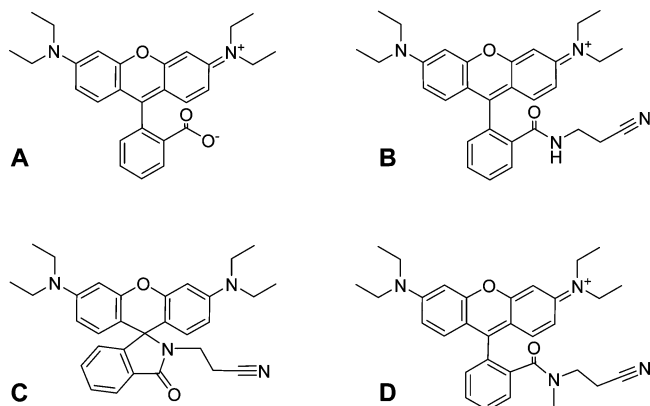
(16) Zayat, L.; Noval, M. G.; Campi, J.; Calero, C. I.; Calvo, D. J.; Etchenique, R. *ChemBioChem* **2007**, *8*, 2035–2038.

(17) Fino, E.; Araya, R.; Peterka, D. S.; Salierno, M.; Etchenique, R.; Yuste, R. *Front. Neural Circuits* **2009**, *3*, 1–10.

(18) Salierno, M.; Marceca, E.; Peterka, D. S.; Yuste, R.; Etchenique, R. *J. Inorg. Biochem.* **2010**, *104*, 418–422.

(19) Viala, C.; Coudret, C. *Inorg. Chim. Acta* **2006**, *359*, 984–989.

Scheme 1. (A) Rhodamine B; (B) RhodB-APN, Fluorescent Form; (C) RhodB-APN, Spirolactame Nonfluorescent Form; (D) RhodB-MAPN



[Ru(bpy)₂(H₂O)Cl]⁺ complex was determined by its band at 490 nm in water. 1.5 equivalents of VACN diluted in 4 mL of EtOH were added and the mixture was kept at 80 °C during 2 h. The solvent was removed by distilling under a vacuum, and the residue was redissolved in 2 mL of water, centrifuged to remove any solid, and precipitated with saturated KPF₆. Yield 66%.

NMR (Acetone-D₆): ¹H δ 3.65 (d, 2H), 5.13 (d, 2H), 5.75 (m, 1H), 7.29 (t, 1H), 7.32 (t, 1H), 7.70 (d, 1H), 7.81 (t, 1H), 7.92 (3t, 3H), 7.97 (d, 1H), 8.20 (t, 1H), 8.31 (t, 1H), 8.56 (d, 1H), 8.60 (d, 1H), 8.69 (d, 1H), 8.74 (d, 1H), 9.53 (d, 1H), 10.08 (d, 1H).

RESULTS AND DISCUSSION

Rhodamines are superb fluorophores, due to their emission quantum yield approaching unity and their high resistance to photobleaching. They are comprised of a xanthene moiety that provides the fluorescence and a benzoic acid which modulates their spectral properties. Scheme 1A shows the structure of rhodamine B which was chosen as the starting point for our work.

Ruthenium–bipyridyl complexes can easily be coordinated to donor nitrogens such as those of the aliphatic amines, pyridines, imines, and even nitriles, but not to those of anilines, not even primary ones. Diethylanilines of the rhodamine B do not form stable complexes with Ru centers and although carboxylates can be coordinated to Ru–bpy cores, such complexes are easily hydrolyzed in aqueous solutions at room temperature.

Given these properties it was necessary to modify the chemical structure of rhodamine B by adding a “sticky tail” in order to coordinate the fluorescent molecule to the metal center. In a first attempt to synthesize a modified rhodamine bearing a coordinating group, we proceeded to the amidation of the carboxylate with aminopropionitrile, using the Adamczyk procedure.²⁰ The obtained compound is RhodB–APN, indicated in scheme 1B. However, although this ligand can be coordinated to Ru–bpy complexes through the nitrile, it undergoes isomerization to the cyclic spirolactame form at physiological pH (scheme 1C) becoming nonfluorescent.

A secondary amide cannot isomerize to the cyclic form, thus RhodB–MAPN, obtained through an amidation of rhodamine B

acid chloride²¹ with aminopropionitrile (Scheme 1D) presents a very high, yellow fluorescence while its terminal nitrile allows its coordination to a Ru–bpy center.

The complex *cis*-[Ru(bpy)₂(L)Cl]PF₆, L = RhodB–MAPN was obtained as a dark purple solid, slightly soluble in water and very soluble in acetone. Due to its very high molar absorptivity, its water solubility is high enough for most experimental situations. For the FIA imaging experiments it was used in this form. A much more soluble chloride salt, which is better for the biological experiments, was prepared by means of batch ion exchange with Dowex 22-Chloride resin in 1:1 acetone–water. The salt was used in biological experiments. The solutions of the complex present a weak yellowish fluorescence. Preliminary studies showed that the complex is light sensitive, increasing its fluorescence when irradiated in aqueous, ethanol or acetone solutions.

Figure 1 shows a TLC sequence prepared from the raw reaction mixture. The TLC plate was run using a 1:1:1 water/EtOH/nBuOH mixture as eluting solvent and silica as stationary phase. The ligand RhodB–MAPN runs with R_f = 0.5, clearly above its Ru complex (R_f = 0.15). A third spot corresponding to the starting complex [Ru(bpy)₂(H₂O)Cl]Cl can be seen at the origin.

The pictures were taken with the following procedure: while illuminating the plate with a green LED (528 nm), and using an orange gelatin filter in front of the camera objective to highlight the fluorescence, the first picture was taken (frame 0). In this conditions, the orange fluorescence of the free ligand is evident, while the other spots remain dark.

Before the second picture was shot (frame 1), a blue light pulse (473 nm) was directed to the rightmost lane during 3 s. After this procedure the spot at R_f = 0.15 became fluorescent under green light. A similar procedure was used to “turn on” the remaining spots before shooting frames 2 and 3. Subsequent running in the same solvent showed that the new, fluorescent substance has R_f = 0.5, corresponding to that of the free ligand RhodB–MAPN (not shown). The identity of the complex and its photoproducts were determined by ¹H NMR.

Figure 2 (top) shows the aliphatic region of the ¹H NMR spectrum of the Ru complex bearing RhodB–MAPN as a ligand, showing the expected number of signals and integrations for a coordinate RhodB–MAPN. The double multiplet at 3.40–3.55 ppm (labeled a') corresponds to the methylene group closest to the coordination point. The triplet at 2.98 ppm (b') and the singlet at 3.10 ppm (c') correspond to the other methylene and the *N*-methyl group respectively. Similar signals were obtained if just the aminonitrile tail is coordinated to the Ru–bpy core. After 5 min of irradiation inside the NMR tube using a 450 nm LED (middle trace), new signals appear at 2.37, 3.16, and 3.53 ppm, due to the release of the RhodB–MAPN ligand. These three signals exactly match those of the free ligand (labeled a, c, and b, respectively, bottom trace). The four ethyl groups of RhodB–MAPN are not totally equivalent, and they are seen as a multiplet (–CH₂–) or broad triplet (–CH₃) and present little change after irradiation since they are far from the coordination center.

(20) Adamczyk, M. J. *Bioorg. Med. Chem. Lett.* **2000**, *10*, 1539–1541, Grote.

(21) Fölling, J.; Belov, V.; Medda, R.; Schönle, A.; Egner, A.; Eggeling, C.; Bossi, M.; Hell, S. W. *Angew. Chem.* **2007**, *46*, 6266–6270.

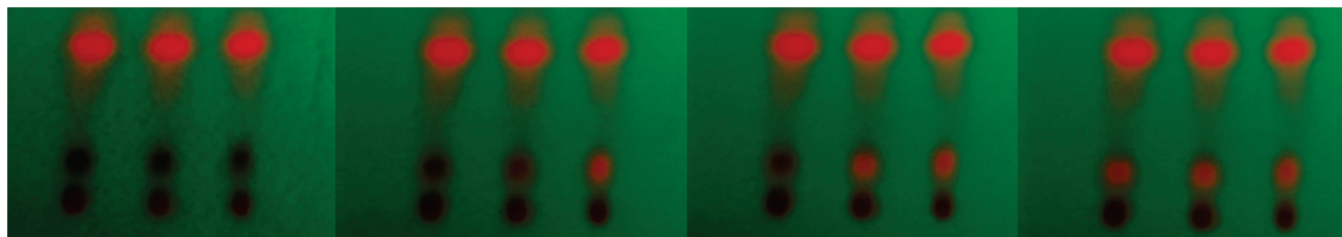


Figure 1. Four sequential photographs of a single TLC plate run of the reaction. The top fluorescent spot ($R_f = 0.5$) is RhodB–MAPN. The lowest, nonfluorescent spot ($R_f \sim 0$) is the starting complex $[\text{Ru}(\text{bpy})_2(\text{H}_2\text{O})\text{Cl}]\text{Cl}$. The middle spot ($R_f = 0.15$) corresponds to the product $[\text{Ru}(\text{bpy})_2(\text{RhodB-MAPN})\text{Cl}]\text{Cl}$. In frame 0 the plate was not irradiated. Irradiation with intense blue light (473 nm) was sequential from left to right, just before frames 1, 2, and 3. Notice the dramatic increase of fluorescence emission from the middle spot after blue-light irradiation. Pictures were taken using a green (528 nm) LED as light source and an orange filter in front of the camera objective.

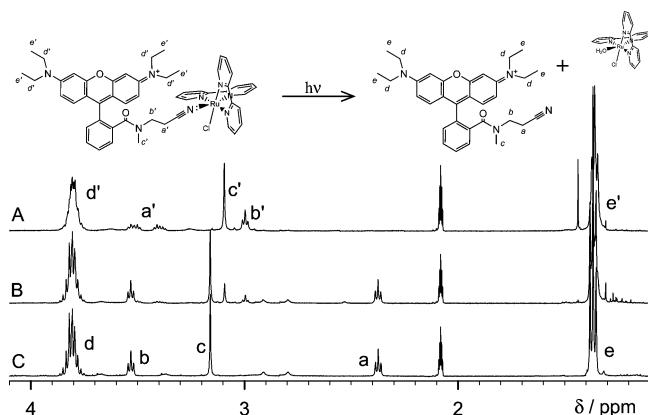


Figure 2. ^1H NMR aliphatic region spectra of the complex $[\text{Ru}(\text{bpy})_2(\text{RhodB-MAPN})\text{Cl}]^+$ (A) before irradiation. (B) after 5 min irradiation. (C) free RhodB–MAPN spectrum. Note in B that the signals of the free ligand **a**, **b**, and **c** are apparent, indicating its photorelease. The signals **d** and **e**, corresponding to the ethyl groups in RhodB–MAPN, are far from the coordination center and therefore do not suffer big changes. A photolysis reaction schematic is added for clarity.

In the aromatic region (See Supporting Information Figure S1) the expected number of signals and integrations for a nonsymmetric *cis* complex¹⁶ bearing RhodB–MAPN were obtained. After photolysis, the signals from the free RhodB–MAPN at 6.98, 7.20, 7.37, 7.62, 7.77, and 7.82 appear at the same chemical shifts as those from aquo-complex $[\text{Ru}(\text{bpy})_2(\text{H}_2\text{O})\text{Cl}]^+$.

Dilute aqueous solutions of $[\text{Ru}(\text{bpy})_2(\text{RhodB-MAPN})\text{Cl}]^+$ present weak fluorescence with a maximum at 592 nm (excitation 518 nm).

Figure 3 depicts the emission spectra of the complex during irradiation. The maximum and the shape of the initial emission spectrum is the same as that of the free ligand RhodB–MAPN but the emission quantum yield is much lower, around $\phi_f = 0.04$. Quantum yields are easily calculated integrating the spectral areas. After irradiation with a 473 nm laser, RhodB–MAPN is released and the solution increases its fluorescence up to 6 fold, to $\phi_f = 0.24$. The inset shows the maxima of the spectra as a function of the irradiation time.

The quantum yield of rhodamine photorelease was calculated after the analysis of fluorescence emission data during photouncaging at 473 nm. A complete spectrum was obtained once every ten seconds. Absorption of light by the complex $[\text{Ru}(\text{bpy})_2(\text{RhodB-MAPN})\text{Cl}]^+$ yields the aquo complex $[\text{Ru}(\text{bpy})_2(\text{H}_2\text{O})\text{Cl}]^+$ and free RhodB–MAPN. In each irradiation period

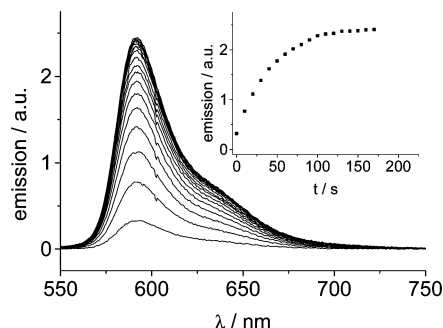


Figure 3. Emission spectra of a 10 μM aqueous solution of the complex $[\text{Ru}(\text{bpy})_2(\text{RhodB-MAPN})\text{Cl}]^+$ during irradiation of the cuvette with a 473 nm laser diode. A spectrum was measured every 10 s. Inset: Emission maxima during irradiation.

the amount of aquo complex and free RhodB–MAPN generated is given by the following:

$$\delta n = \delta t I \phi_{\text{PU}} (1 - 10^{-\text{Abs}_R}) \text{Abs}_R / \text{Abs}_T$$

Where δt is the irradiation period, I the light intensity in moles of photons per second, ϕ_{PU} is the quantum yield of photouncaging, Abs_R is the absorbance of the photoactive species $[\text{Ru}(\text{bpy})_2(\text{RhodB-MAPN})\text{Cl}]^+$ at 473 nm and Abs_T is the total absorbance of the irradiated solution. By means of finite element calculation of the former equation a photouncaging quantum yield of $\phi_{\text{PU}} = 0.12$ at 25 $^\circ\text{C}$ was calculated. This value is in good agreement with the reported quantum yields for similar complexes.^{14–16}

The origin of this quenching can be attributed to the presence of the nearby ruthenium–bipyridine moiety, which presents an MLCT transition which overlaps with that of the rhodamine emission. However, direct inspection of the absorption bands of this complex at such a wavelength range is impossible, due to the very high molar extinction of the fluorescent ligand (ca., $10^5 \text{ M}^{-1}\text{cm}^{-1}$), which obscures any absorption due to the metal center.

In order to measure this absorption, an analogous complex was synthesized using vinylacetonitrile (VACN) instead of RhodB–MAPN. It is very known that the energy of the MLCT band of the Ru–bpy complexes are strongly dependent on the nature and basicity of the ligands near the Ru center,²² but almost independent of the farther fragments. The complex $[\text{Ru}(\text{bpy})_2(\text{VACN})\text{Cl}]^+$ shows the typical MLCT band, which

(22) Pinnick, D. V.; Durham, B. *Inorg. Chem.* **1984**, *23*, 1440–1445.

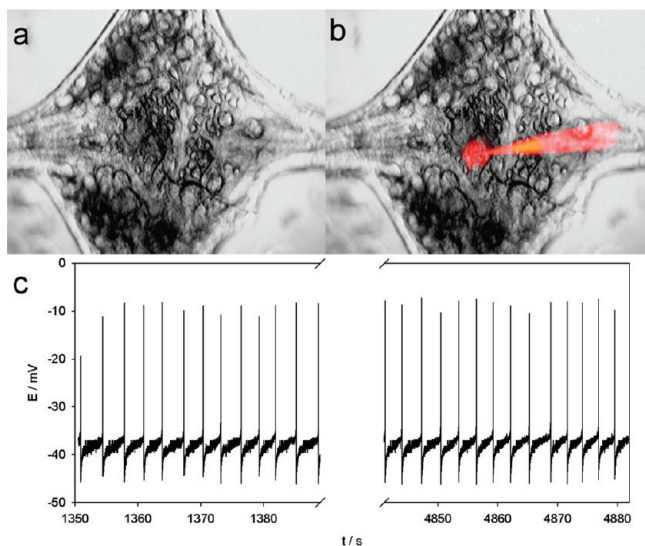


Figure 4. (a) Leech ganglion imaged in infrared. (b) Fluorescence image of a Retzius neuron being filled with $[\text{Ru}(\text{bpy})_2\text{-(RhodB-MAPN)Cl}]^+\text{Cl}^-$ through a sharp microelectrode. (c) Action potentials of the Retzius neuron are not affected by the injection.

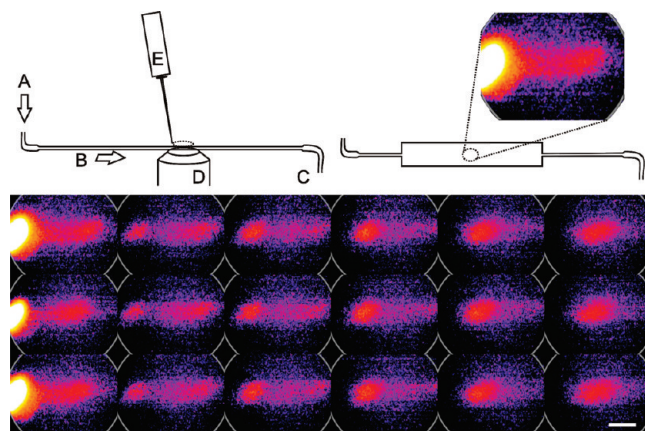


Figure 5. Top: schematics of the planar flow cell photolysis device. The inlet and outlet tubing (A,C) guide the flow through a planar flow cell (B) where it is photolyzed by a 405 nm violet laser (E) and monitored through a $10\times$ objective (D). Bottom: selected images from the video sequence recorded at 400 frames/s showing fluorescence intensity in false color. Velocity: 2 cm/s. Scale bar represents 500 μm .

is centered around 460 nm and extends more than 100 nm to the low energy region, overlapping with the emission spectra of the rhodamine ligand. This absorption is enough to explain the observed quenching. This analog complex photoreleases VACN with even a higher quantum yield of $\phi_{\text{PU}} = 0.21$.

As the caged fluorescent probe is a useful tool to investigate cellular mechanisms at the cellular level, its toxicity must be evaluated. Neurons are excitable cells that change their properties dramatically when exposed to toxic substances. Direct injection and uncaging of the complex inside a neuron is a useful test for evaluating acute cellular toxicity. Figure 4a shows a leech neuronal ganglion imaged in infrared, composed by about 400 neurons. Two of these neurons, named Retzius cells, regularly spike action potentials. Figure 4b shows superimposed in a fluorescence image the injection of the complex from an impaled sharp capillary

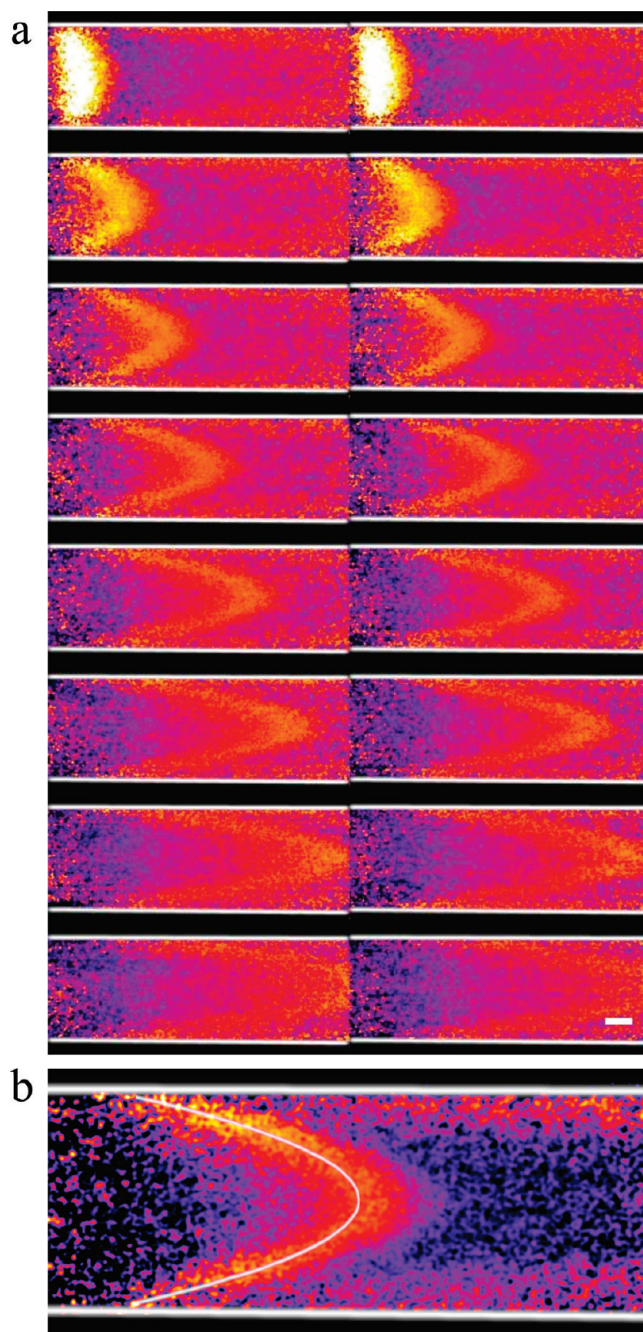


Figure 6. (a) Flow through a FIA capillary recorded using $[\text{Ru}(\text{bpy})_2(\text{RhodB-MAPN)Cl}]\text{PF}_6^-$ as a probe and depicted in false color. Scale bar represents 200 μm . (b) Flow showing the parabolic plume. Maximum velocity: 4.5 mm/s.

microelectrode (tip diameter $< 1\ \mu\text{m}$) filled with physiological saline solution containing 1 mM of the complex. The spiking behavior of the neuron did not change as a result of the injection and uncaging procedures ($n = 6$), remaining normal as can be seen in Figure 4c. The cells continued spiking during several hours, showing no difference with the Retzius neurons which were not treated with the complex. The fluorescence remained inside the boundaries of the cell, and no leakage was detected.

The dynamic imaging capabilities of the fluorescent probe were tested in two models: a thin, planar 2D flow cell and a FIA-sized capillary. Figure 5 (top) shows the schematics of the plane flow cell and its dimensions. A 405 nm, 6 mW laser diode was

controlled with a pulse generator using a fast Reed relay to provide 20 ms light pulses. The laser beam was focused to the cell plane and monitored with an inverted microscope (Nikon TS100 w/fluorescence adapter). The use of visible light pulses from a diode allows the possibility of high repetitive rate measurements with inexpensive components.

The sequence of images in Figure 5 (bottom) shows that the fluorescent spot generated by means of the pulse keeps its dimensions and shape through the entire path in the cell, indicating laminar flow. However, some spreading is also apparent, due to the diffusion and to the viscous interaction of the spot with the bottom and top faces of the cell. Full video is available as Supporting Information.

One of the most important problems of the pressure-driven FIA and similar systems arise from the parabolic flow that results from the viscous interactions of the fluid with the capillary walls. Figure 6a shows a frame sequence of a FIA sized capillary imaged with a similar system, in which a 20 μ s laser pulse activates a thin slice of caged rhodamine. The uncaged spot becomes a parabolic plume immediately and travels through the capillary as can be seen in the subsequent frames. The velocity profiles can be precisely recovered by means of a simple frame by frame analysis and follows the expected quadratic behavior.

A parabola can be well fitted to the flow shape, and the velocity profile can be calculated as can be seen in Figure 6b, being $v_{\max} = 4.5$ mm/s. The repetitive pulses allow the visualization of a very slow analyte tail near the walls of the cell, which can result in signal broadening in FIA systems and memory effect.

In conclusion, we have devised a new tool: The first activatable fluorescent probe with sensitivity in the visible light region. It increases its intrinsic fluorescence up to 6 fold after blue light irradiation. This probe is physiologically friendly and can be injected into living cells—even excitable ones like neurons—with no sign of acute toxicity in short-term (~ 2 h) experiments. The probe was used to image the laminar flow inside a thin spectrophotometric flow cell and to visualize the parabolic-shaped flow in a FIA capillary. This probe reveals not only the broadening of the plume, but also the memory effect due to accumulation of analyte near the walls, where the flow velocity approaches zero. In brief, the complex $[\text{Ru}(\text{bpy})_2(\text{RhodB}-\text{MAPN})\text{Cl}]^+$ is a superb tool to image any kind of systems where manipulation of fluorescence is required.

ACKNOWLEDGMENT

We thank Dr. Sara Maldonado for her invaluable help, and Dr. Lidia Szczupak for kindly providing us with leeches. This research was supported by the National Agency for Science and Technology Promotion and the University of Buenos Aires. R.E. is a staff member of CONICET.

SUPPORTING INFORMATION AVAILABLE

NMR spectra of the Rhodamine complex and Videos corresponding to the data depicted in Figures 5 and 6. This material is available free of charge via the Internet at <http://pubs.acs.org>.

Received for review May 7, 2010. Accepted June 14, 2010.

AC1012128